



Supporting Online Material for

Evolution of Hormone-Receptor Complexity by Molecular Exploitation

Jamie T. Bridgham, Sean M. Carroll, Joseph W. Thornton*

*To whom correspondence should be addressed. E-mail: joet@uoregon.edu

Published 7 April 2006, *Science* **312**, 97 (2006).

DOI: 10.1126/science.1123348

This PDF file includes

Materials and Methods

Figs. S1 to S7

Tables S1 to S4

References and Notes

Contents

- Methods
- Figure S1. Complete maximum likelihood phylogeny of steroid receptors.
- Figure S2. Complete BMCMC phylogeny of steroid receptors.
- Figure S3. Complete maximum parsimony phylogeny of steroid receptors.
- Figure S4. Dose-response relationships for hagfish and lamprey CR-LBDs with adrenal steroids.
- Figure S5. Full-length hagfish CR is aldosterone-activated.
- Figure S6. Alternative reconstructions of the ancestral CR are activated by aldosterone.
- Figure S7. Aldosterone is not produced in cultured lamprey and hagfish interrenal glands.
- Table S1. Sequences, species and accession numbers used for phylogeny and ancestral reconstruction.
- Table S2. Maximum likelihood sequence and site-specific posterior probabilities for the ancestral corticoid receptor LBD.
- Table S3. Amino acid sequence identify of AncCR to extant corticosterone receptors.
- Table S4. Effects of GR-diagnostic residues on ligand activation of AncSR4-LBD.
- References for supplemental information.

METHODS

Corticoid receptor isolation. RNA was isolated from the livers of hagfish *Myxine glutinosa* and skate *Raja erinacea* using RNeasy kit (Qiagen, Valencia, CA). cDNAs were generated using Thermoscript enzyme (Invitrogen, Carlsbad, CA) and oligo-dT primers. Degenerate PCR to identify partial CR sequences was conducted using primers based on the conserved DNA-binding and ligand-binding domains (DBD and LBD) of vertebrate GRs and MRs. Nested rapid amplification of cDNA ends (RACE) was conducted using the SMART-RACE kit (BD Biosciences, Palo Alto, CA). *Petromyzon marinus* CR was previously isolated (1). GR and MR of *Rattus norvegicus* and GR2a and MR of *Astatotilapia burtoni* were provided by D. Pearce and R. Fernald, respectively.

Receptor characterization. Receptor LBDs (including the hinge region and carboxy-terminal extension) were amplified by high-fidelity PCR and cloned into a GAL4-DBD-pSG5 expression vector (gift of D. Furlow). The LBD is a functionally separable domain that contains the protein's ligand-regulated transcriptional functions (2). 1 ng of receptor plasmid, 100 ng of a UAS-driven firefly luciferase reporter (pFRluc), and 0.1 ng of the constitutive phRLtk *Renilla* luciferase reporter were transfected into Chinese hamster ovary (CHO-K1) in 96-well plates using Lipofectamine Plus in OPTIMEM (Invitrogen). After 4 hours, transfection medium was replaced with phenol-red-free α MEM supplemented with 10% dextran-charcoal-stripped fetal bovine serum (Hyclone). After overnight recovery, cells were incubated in triplicate with hormone for 24 hours, then assayed by luminometry using the Dual-Glo luciferase system (Promega, Madison, WI). Firefly luciferase activity was normalized by *Renilla*

luciferase activity; dose-response relationships were estimated using non-linear regression in Prism4 software (GraphPad Software, Inc., San Diego, CA). The full-length hagfish CR cDNA was cloned into pcDNA3 (Invitrogen), and co-transfected into CV-1 (African green monkey kidney fibroblast) cells with the TAT3luc reporter, which contains tandem glucocorticoid response elements, as described above.

Hormone identification. Blood was collected from 17 hagfish and 14 lampreys using heparinized syringes. Plasma samples from each species were pooled after centrifugation. For each species 2 ml of plasma was extracted 1:5 with dichloromethane, dried and resuspended in 200 μ l of 50% methanol. Reverse phase HPLC was performed on an Agilent 1100 Diode Array Detector 1, with an Agilent Zorbax C18 column (Palo Alto, CA), at 0.200ml/min with an isocratic elution using 50% methanol in water as solvent. The elution profile was monitored at 240nm, and the aldosterone peak position was verified using spiked plasma controls (spiked with 500pg/ml prior to extraction). Four-minute fractions were collected, dried and resuspended in 0.35 ml EIA buffer. An aldosterone enzyme-linked immunoassay (EIA) kit (Cayman Chemical, Ann Arbor, MI) was used to analyze each HPLC fraction in triplicate. A standard curve from 7.8 to 1000 pg/ml hormone was established for each assay. The limit of detection was calculated as 80% of total minus non-specific binding on controls per manufacturer's instructions. For explant incubation experiments, interrenal tissues were isolated from three hagfish and three lampreys and incubated as described(3) in 500 μ l buffered saline supplemented with lamprey ACTH(3) and 100nM corticosterone for 6 hours with shaking at 18°C for lamprey and 4°C for hagfish. Medium was collected and extracted, HPLC fractionated, and EIA-analyzed as described above.

Phylogenetic analysis. 59 steroid receptor protein sequences (for accessions, see Table S1) were aligned using ClustalX software (4) assuming the Gonnet replacement matrix and gap:change cost 8. Phylogeny was inferred by BMCMC analysis using MrBayes v. 3.0b4 (5) by integrating over protein models, assuming a four-category gamma ASRV distribution, with uniform priors over trees, branch lengths (0,5), and the ASRV alpha parameter (0.05-10). Three independent analyses, each with four chains (three heated), were run for 300,000 generations and sampled every 100 generations; the first 500 samples from each run, a point well past stationarity, were discarded as burn-in. All analyses converged on the same tree and found the JTT protein model had 100% posterior probability. Phylogeny was also inferred by ML using a novel implementation that searches tree space using simulated annealing optimization of topology and branch lengths; 2000 temperatures were evaluated from 1 to 1e-6, with 1000 iterations per temperature, and an acceptance ratio of 0.3, assuming the JTT protein model and a 4-category discrete gamma distribution of among-site rate variation (ASRV). For parsimony analysis, we used PAUP* 4.0b10 and a stepmatrix derived from the Gonnet empirical model of protein replacement probabilities (1). A heuristic search of 100 replicates of random addition plus tree-bisection-reconnection branch swapping was used; to estimate support, 100 bootstrap replicates were analyzed using 10 replications of random addition/TBR each.

Ancestral sequence reconstruction. Sequences at internal nodes on the phylogeny were inferred by ML(6) using PAML v.3.14, assuming gamma-distributed ASRV and the JTT protein model. Sequences were reconstructed assuming the ML tree, the 50% Bayesian consensus tree. To determine the robustness of the ancestral inference

to uncertainty about phylogeny, we used BMCMC to collect a large sample of trees and independently reconstructed the ancestral sequence using PAML on each of the 467 trees in the 95% credible set from the BMCMC analysis. A cDNA coding for the inferred AncCR LBD+CTE was synthesized (Genscript, Piscataway, NJ) and verified by sequencing, then cloned into Gal4-DBD-pSG5. Hormone-regulated transcriptional activity was assayed in CHO-K1 cells as described above. Variant receptors were constructed by site-directed mutagenesis using Quikchange (Stratagene) and verified by sequencing.

Figure S1. Complete maximum likelihood phylogeny. The tree is rooted to minimize gene duplications; other rootings require additional duplications and losses. The corticoid receptors are shown in bold. AncCR is marked with a dark circle. For analysis methods and parameters, see Methods.

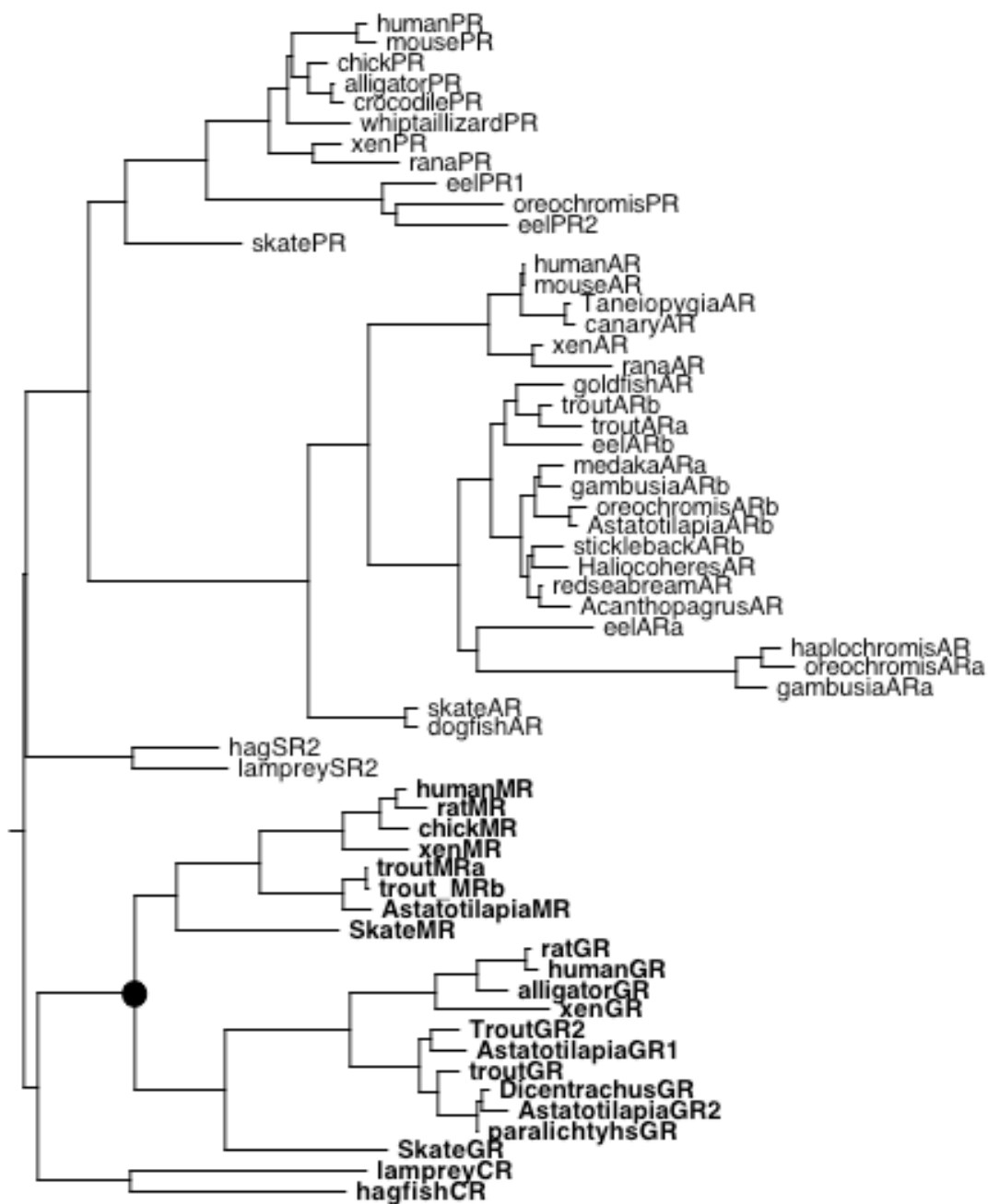


Figure S2. Complete BMCMC phylogeny. Branch labels indicate posterior probabilities. The tree is rooted to minimize gene duplications; other rootings require additional duplications and losses. Corticoid receptors in bold. Dark circle, AncCR. For analysis parameters, see Methods.

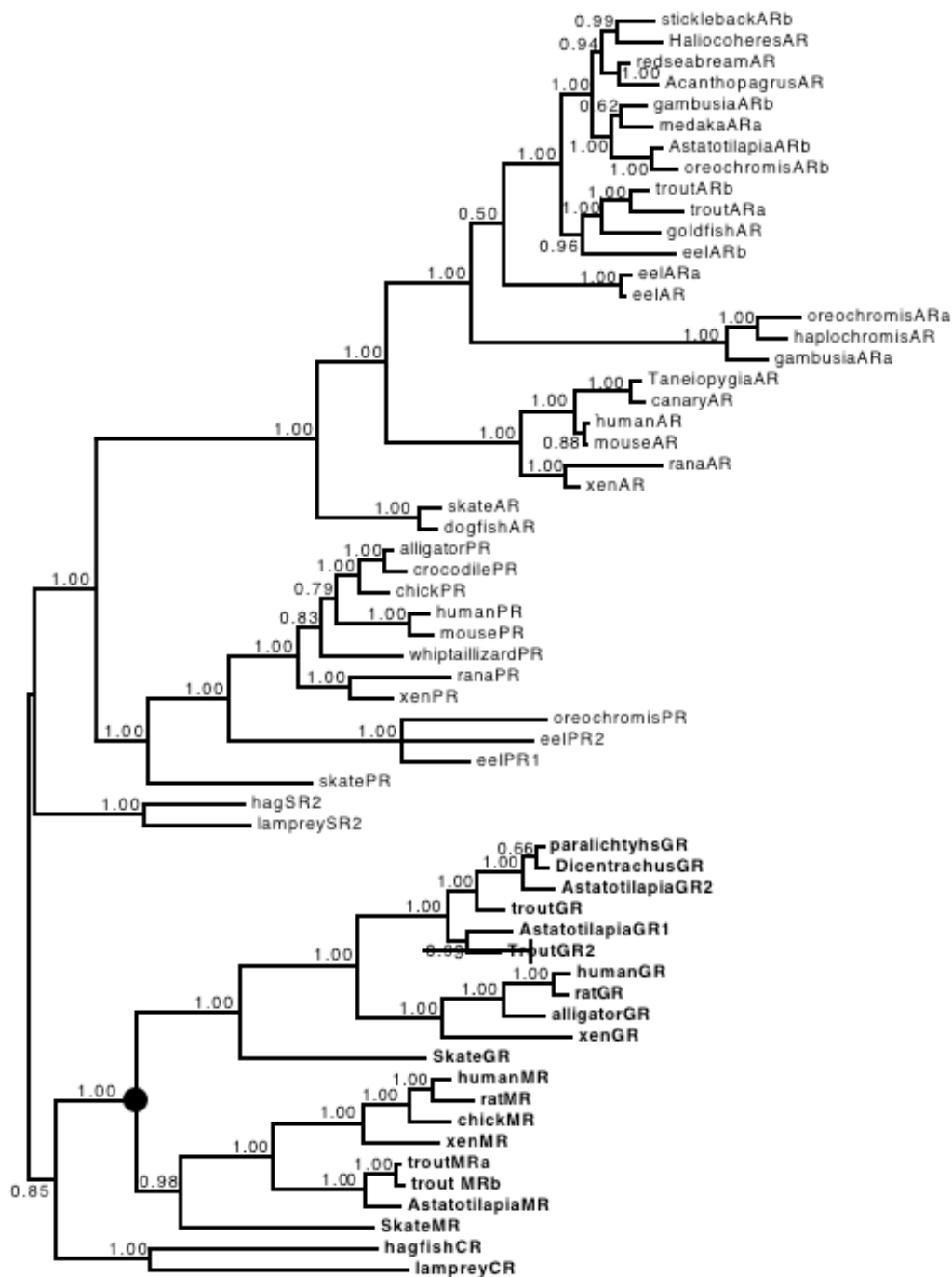


Figure S3. Complete maximum parsimony phylogeny. Branch labels indicate bootstrap percentages. The tree is rooted to minimize gene duplications; other rootings require additional duplications and losses. For analysis parameters, see Methods.

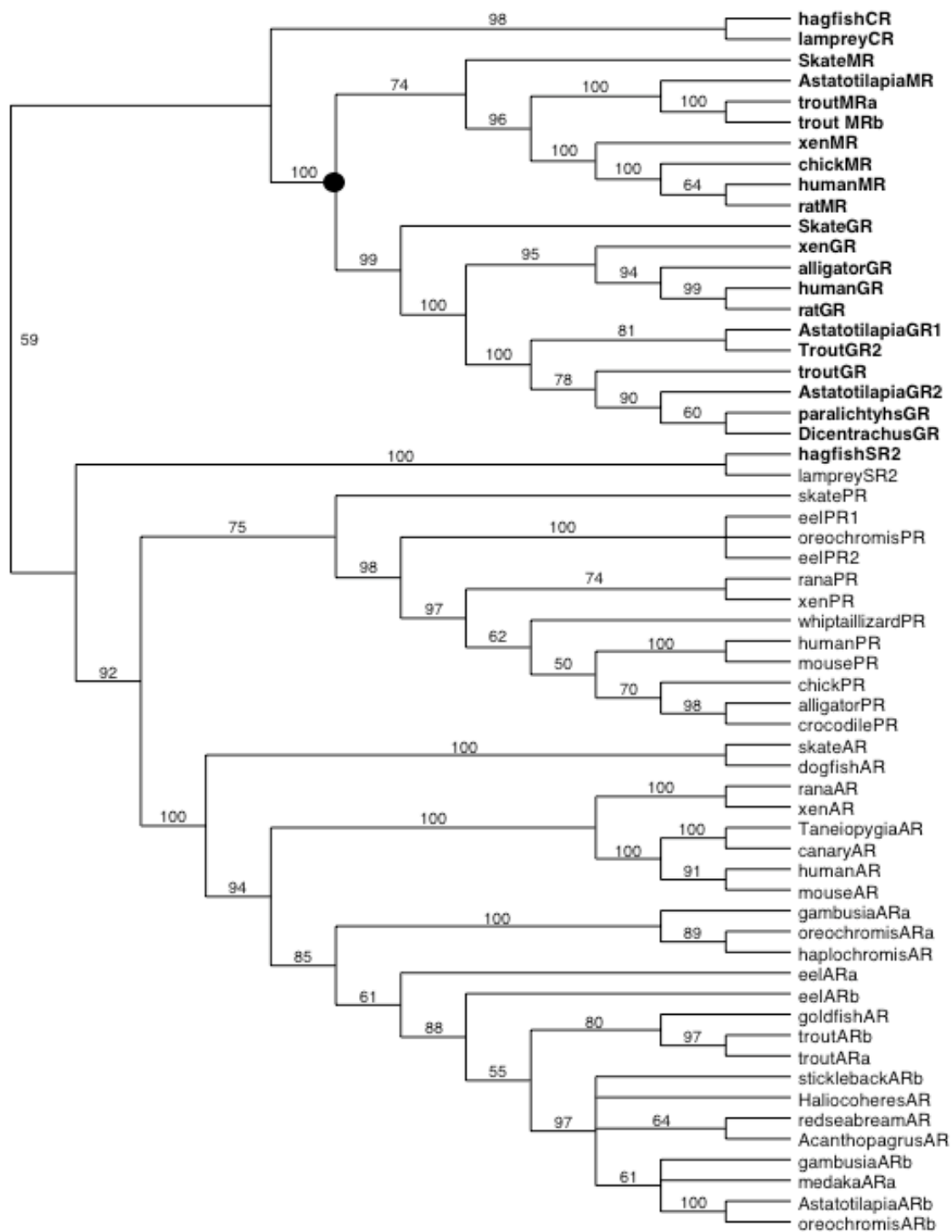


Figure S4. Dose-response relationships for hagfish and lamprey CR-LBDs with adrenal steroids. Fold-increase in activation of a UAS-driven luciferase reporter gene by each receptor is shown as the hormone dose increases. Errors bars shown s.e.m. for three replicates.

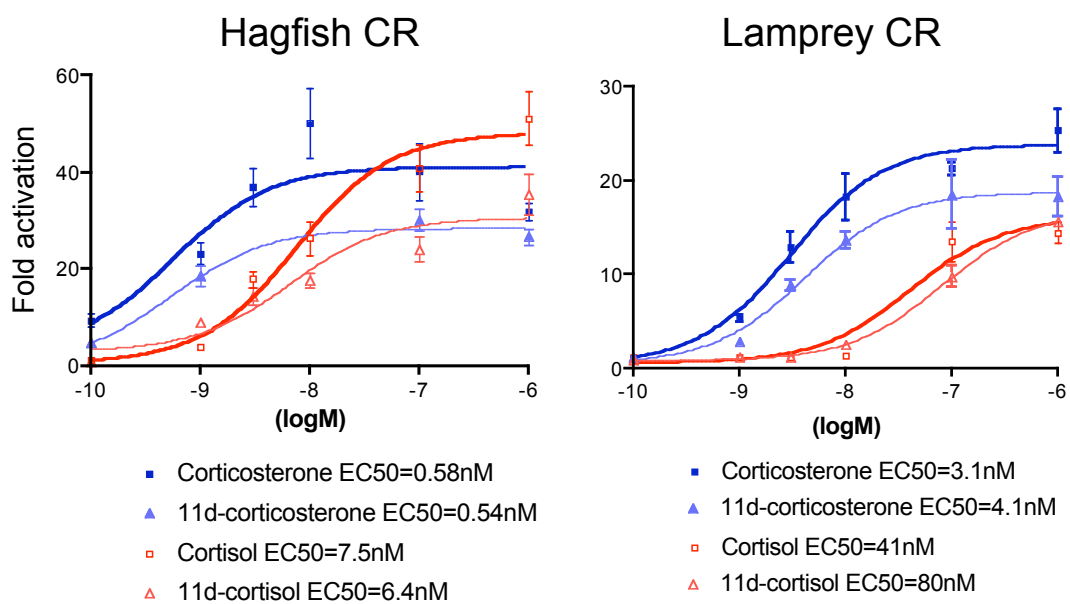
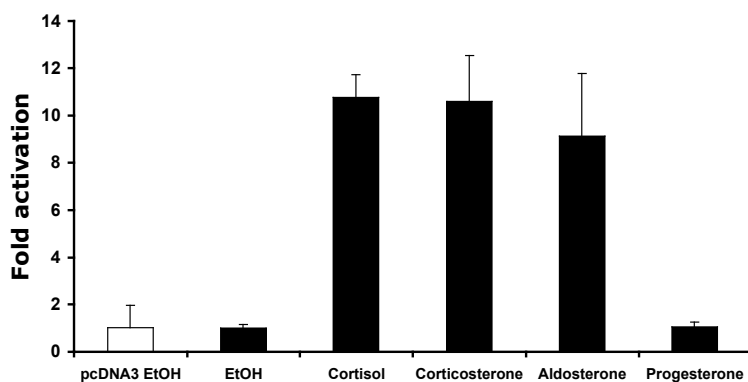


Figure S5: Full-length hagfish CR is aldosterone-activated. The full-length hagfish CR was cloned into pcDNA3 mammalian expression vector and transformed into CV-1 cells along with the TAT3-luc reporter plasmid containing a GRE promoter. A) Luciferase activation, expressed as fold-increase over vehicle only, are shown for treatments with 100nM cortisol, corticosterone, aldosterone or progesterone. B) Luciferase activity dose-response with increasing aldosterone concentrations ($EC_{50} = 0.39\text{nM}$). Data are expressed as fold activation relative to vehicle controls.

A)



B)

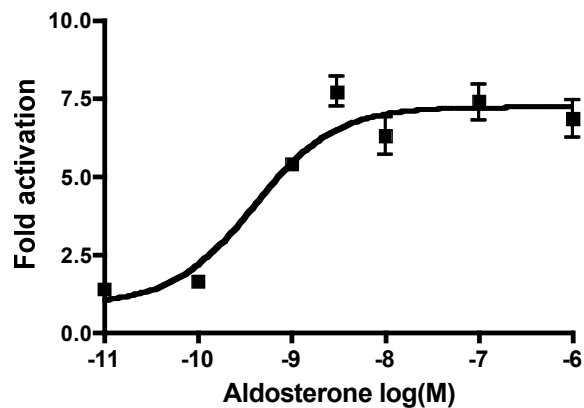
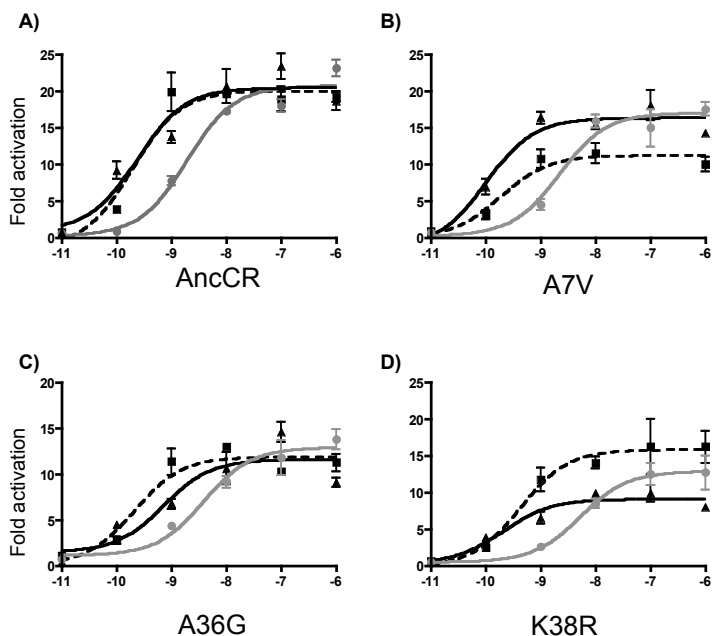


Figure S6. Alternative reconstructions of the ancestral CR are activated by aldosterone. AncCR-LBD was subject to directed mutagenesis to introduce alternative reconstructions; these constructs were then assayed for hormone-activated expression of a luciferase reporter gene, shown as fold-increase in normalized activity compared to vehicle control. Aldosterone, squares and black line; 11-deoxycorticosterone, triangles and dotted line; cortisol, circles and gray line. A) Unmutagenized maximum-likelihood reconstruction of the AncCR-LBD. B) Site 7 was the only position with an alternative ML state (V instead of A) due to uncertainty in the phylogeny. C) A36G introduces the only alternative reconstruction due to statistical uncertainty (posterior probability >0.20) at sites in the ligand binding pocket based on the human MR structure. D) K38R introduces the only alternative reconstruction in the entire LBD that is not found in aldosterone-activated receptors. EC50s with aldosterone (aldo), cortisol (cort) and 11-DOC (DOC) are shown below. These data indicate that this function of the ancestor is robust to alternative sequence reconstructions, consistent with results from other studies (7). Sites are numbered by position in the AncCR-LBD (see Table S2).



A) AncSR4 Aldo EC50 = 0.23nM; Cort EC50 = 5.6nM; DOC EC50 = 0.19nM

B) A7V Aldo EC50 = 0.1nM; Cort EC50 = 2.1nM; DOC EC50 = 0.18nM

C) A36G Aldo EC50 = 0.7nM; Cort EC50 = 3.8nM; DOC EC50 = 0.2nM

D) K38R Aldo EC50 = 0.2nM; Cort EC50 = 5.2nM; DOC EC50 = 0.4nM

Figure S7. Aldosterone is not produced in cultured lamprey and hagfish interrenals. Lamprey and hagfish interrenal explants were incubated with corticosterone – the precursor of aldosterone – and adrenocorticotrophic hormone, which stimulates interrenal steroid hormone synthesis, and the liquid medium was then assayed for aldosterone by HPLC followed by EIA. **Top,** HPLC chromatogram of aldosterone-spiked lamprey plasma. The peak represents retention time for aldosterone. **Bottom,** Enzyme-linked immunoassay for aldosterone on HPLC-separated fractions of medium from incubated explants. The limit of detection is shown as a solid line. A similar experiment using aldosterone-spiked lamprey plasma (Fig. 3B in the main text) demonstrates the capacity of this HPLC-EIA procedure to detect aldosterone. However, we cannot rule out the possibility that the absence of aldosterone from the treated explant cultures might be a negative artifact due to a failure of the explants to respond to ACTH.

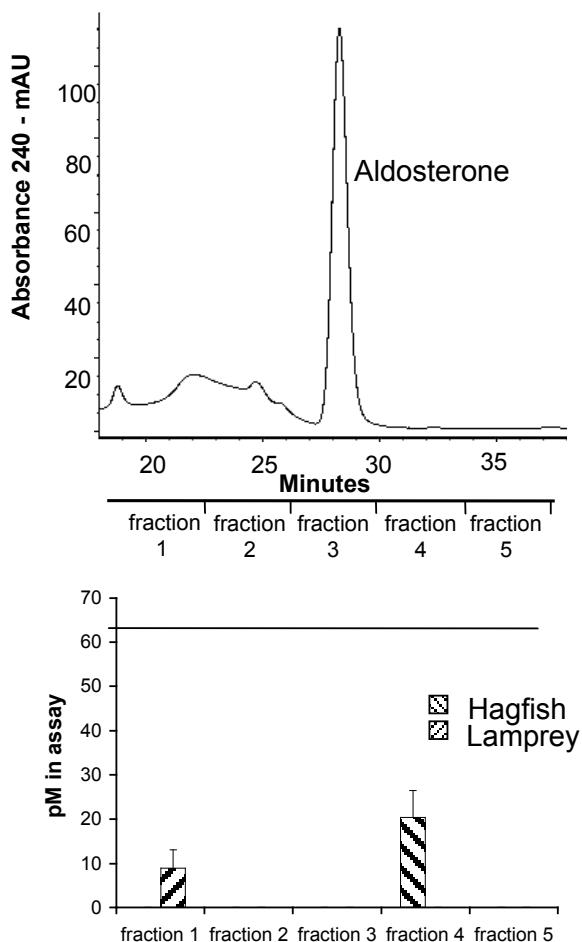


Table S1. Sequences, species, and accession numbers used in the steroid receptor phylogeny and ancestral sequence inference.

Sequence name (on phylogeny)	Genbank ID	Species
AcanthopagrusAR	28974723	<i>Acanthopagrus schlegelii</i>
AlligatorGR	22135433	<i>Alligator mississippiensis</i>
AlligatorPR	41386653	<i>Alligator mississippiensis</i>
AstatilapiaARb	19879685	<i>Astatotilapia burtoni</i>
AstatotilapiaGR1	20563131	<i>Astatotilapia burtoni</i>
AstatotilapiaGR2	20563133	<i>Astatotilapia burtoni</i>
AstatotilapiaMR	20563137	<i>Astatotilapia burtoni</i>
CanaryAR	414734	<i>Serinus canaria</i>
ChickMR	30315964	<i>Gallus gallus</i>
ChickPR	130893	<i>Gallus gallus</i>
CrocodilePR	2564207	<i>Crocodylus siamensis</i>
DicentrachusGR	44889863	<i>Dicentrarchus labrax</i>
DogfishAR	37909992	<i>Squalus acanthias</i>
EelARa	7446192	<i>Anguilla japonica</i>
EelARb	5821400	<i>Anguilla japonica</i>
EelPR1	6716126	<i>Anguilla japonica</i>
EelPR2	19386568	<i>Anguilla japonica</i>
GambusiaARa	56783596	<i>Gambusia affinis</i>
GambusiaARb	56783598	<i>Gambusia affinis</i>
GoldfishAR	20135660	<i>Carassius auratus</i>
HagfishCR	DQ382336	<i>Myxine glutinosa</i>
HagfishSR2	DQ382337	<i>Myxine glutinosa</i>
HalichoeresAR	12061008	<i>Halichoeres trimaculatus</i>
HaplochromisAR	4583413	<i>Astatotilapia burtoni</i>
HumanAR	4557331	<i>Homo sapiens</i>
HumanGR	121069	<i>Homo sapiens</i>
HumanMR	126885	<i>Homo sapiens</i>
HumanPR	4505767	<i>Homo sapiens</i>
LampreyCR	13919634	<i>Petromyzon marinus</i>
LampreySR2	13919636	<i>Petromyzon marinus</i>
MedakaARa	37359712	<i>Oryzias latipes</i>
MouseAR	113831	<i>Mus musculus</i>
MousePR	130895	<i>Mus musculus</i>
OreochromisARa	12248398	<i>Oreochromis niloticus</i>
OreochromisARb	12248400	<i>Oreochromis niloticus</i>
OreochromisPR	31339298	<i>Oreochromis niloticus</i>
ParalichthysGR	6016116	<i>Paralichthys olivaceus</i>
RanaAR	46576435	<i>Rana catesbeiana</i>
RanaPR	46577033	<i>Rana dybowskii</i>
RatGR	19343485	<i>Rattus norvegicus</i>
RatMR	126886	<i>Rattus norvegicus</i>
RedseabreamAR	3668185	<i>Pagrus major</i>
SkateAR	DQ382340	<i>Raja erinacea</i>
SkateGR	DQ382338	<i>Raja erinacea</i>
SkateMR	DQ382339	<i>Raja erinacea</i>
SkatePR	DQ382341	<i>Raja erinacea</i>
SticklebackARb	29568404	<i>Gasterosteus aculeatus</i>
TaeniopygiaAR	22417219	<i>Taeniopygia guttata</i>
TroutARa	3551156	<i>Oncorhynchus mykiss</i>

TroutARb	3551158	<i>Oncorhynchus mykiss</i>
TroutGR1	1730254	<i>Oncorhynchus mykiss</i>
TroutGR2	40548814	<i>Oncorhynchus mykiss</i>
TroutMRa	53766435	<i>Oncorhynchus mykiss</i>
TroutMRb	53766437	<i>Oncorhynchus mykiss</i>
WhiptaillizardPR	1195594	<i>Cnemidophorus uniparens</i>
XenopusAR	4038480	<i>Xenopus laevis</i>
XenopusGR	1730255	<i>Xenopus laevis</i>
XenopusMR	2500914	<i>Xenopus laevis</i>
XenopusPR	11991857	<i>Xenopus laevis</i>

Table S2. Maximum likelihood sequence and site-specific posterior probabilities for the ancestral corticoid receptor LBD. This sequence has Genbank accession DQ382342.

site	ML state	PP	aligned LB humMR P?	aligned site	Second best state (if > 0.2)	PP of alternative state	Aldosterone-activated receptors with alternative state
1	L	0.919		738			
2	I	0.716		739	V	0.27	humanMR
3	S	0.989		740			
4	I	0.919		741			
5	L	1.000		742			
6	E	0.984		743			
7	A	0.334		744	V	0.31	hagfishCR
8	I	1.000		745			
9	E	1.000		746			
10	P	1.000		747			
11	E	0.991		748			
12	V	0.973		749			
13	V	0.987		750			
14	Y	1.000		751			
15	A	0.999		752			
16	G	1.000		753			
17	Y	1.000		754			
18	D	1.000		755			
19	N	0.684		756	S		humanMR, skateMR, skateGR
20	S	0.772		757	T		lampreyCR
21	Q	0.992		758			
22	P	1.000		759			
23	D	0.998		760			
24	T	1.000		761			
25	T	0.909		762			
26	N	0.971		763			
27	Y	0.615		764	H	0.37	HaplochromisMR
28	L	1.000		765			
29	L	0.999		766			
30	S	0.990		767			
31	S	0.999		768			
32	L	1.000	1	769			
33	N	1.000	1	770			
34	R	0.992		771			
35	L	1.000	1	772			
36	A	0.580	1	773	G	0.30	skateGR
37	G	0.665		774	E	0.33	hagfishCR, skateGR
38	K	0.677		775	R	0.32	0
39	Q	1.000	1	776			
40	M	0.993		777			
41	V	0.933		778			
42	S	0.564		779	R	0.32	HaplochromisMR, skateMR

43	V	0.993		780			
44	V	1.000		781			
45	K	1.000		782			
46	W	1.000		783			
47	A	1.000		784			
48	K	1.000		785			
49	A	0.814		786			
50	L	1.000		787			
51	P	1.000		788			
52	G	1.000		789			
53	F	1.000		790			
54	R	1.000		791			
55	N	0.974		792			
56	L	0.999		793			
57	H	0.996		794			
58	L	0.968		795			
59	D	0.998		796			
60	D	1.000		797			
61	Q	1.000		798			
62	M	1.000		799			
63	T	1.000		800			
64	L	1.000		801			
65	I	0.743		802	L	0.26	skateMR, skateGR
66	Q	1.000		803			
67	Y	1.000		804			
68	S	1.000		805			
69	W	1.000	1	806			
70	M	1.000	1	807			
71	C	0.676		808	S	0.22	skateGR
72	L	1.000	1	809			
73	M	1.000	1	810			
74	A	0.733		811			
75	F	1.000		812			
76	S	0.753		813	A	0.24	lampreyCR, hagfishCR, humanMR
77	L	0.981	1	814			
78	G	0.843		815			
79	W	1.000		816			
80	R	1.000	1	817			
81	S	1.000		818			
82	Y	1.000		819			
83	K	0.998		820			
84	H	1.000		821			
85	T	0.951		822			
86	N	1.000		823			
87	G	0.996		824			
88	Q	0.849		825			
89	M	1.000		826			
90	L	1.000		827			
91	Y	0.999		828			

92	F	1.000	1	829			
93	A	1.000		830			
94	P	1.000		831			
95	D	1.000		832			
96	L	1.000		833			
97	I	0.921		834			
98	F	1.000		835			
99	N	1.000		836			
100	E	1.000		837			
101	E	0.540		838	Q	0.46	HagfishCR, skateMR, skateGR
102	R	1.000		839			
103	M	1.000		840			
104	Q	0.997		841			
105	Q	0.995		842			
106	S	1.000		843			
107	A	0.977		844			
108	M	1.000	1	845			
109	Y	1.000		846			
110	D	0.859		847			
111	L	1.000	1	848			
112	C	1.000		849			
113	Q	0.825		850			
114	G	0.999		851			
115	M	1.000	1	852			
116	R	0.533		853	Q	0.43	skateMR
117	Q	0.932		854			
118	I	0.994		855			
119	S	0.999		856			
120	Q	0.477		857			
121	E	0.997		858			
122	F	1.000		859			
123	V	0.899		860			
124	R	0.991		861			
125	L	1.000		862			
126	Q	1.000		863			
127	V	0.937		864			
128	T	0.934		865			
129	Y	0.645		866			
130	E	0.979		867			
131	E	1.000		868			
132	F	0.963		869			
133	L	1.000		870			
134	C	1.000		871			
135	M	1.000		872			
136	K	1.000		873			
137	V	0.749		874	A	0.25	lampreyCR, hagfishCR, skateGR
138	L	1.000		875			
139	L	1.000		876			
140	L	1.000		877			

141	L	1.000	878			
142	S	0.994	879			
143	T	1.000	880			
144	V	0.819	881			
145	P	1.000	882			
146	K	0.987	883			
147	D	0.865	884			
148	G	1.000	885			
149	L	1.000	886			
150	K	1.000	887			
151	S	0.999	888			
152	Q	1.000	889			
153	A	0.968	890			
154	S	0.397	891	A	0.31	humanMR, HaplochromisMR
155	F	1.000	892			
156	D	0.969	893			
157	E	1.000	894			
158	M	0.997	895			
159	R	1.000	896			
160	M	0.992	897			
161	N	0.977	898			
162	Y	1.000	899			
163	I	1.000	900			
164	K	0.978	901			
165	E	1.000	902			
166	L	1.000	903			
167	O	0.483	904	G	0.34	skateGR
168	R	0.827	905			
169	A	0.688	906	V	0.31	skateMR
170	I	0.951	907			
171	A	0.615	908	V	0.24	skateGR
172	K	0.842	909			
173	K	0.546	910	R	0.33	skateGR
174	E	0.967	911			
175	N	0.827	912			
176	N	1.000	913			
177	S	0.898	914			
178	S	0.539	915	G	0.29	humanMR, HaplochromisMR, skateMR
179	Q	1.000	916			
180	N	0.699	917	S	0.27	humanMR
181	W	1.000	918			
182	Q	1.000	919			
183	R	1.000	920			
184	F	1.000	921			
185	Y	0.999	922			
186	Q	1.000	923			
187	L	1.000	924			
188	T	1.000	925			
189	K	0.998	926			

190	L	1.000		927			
191	L	1.000		928			
192	D	1.000		929			
193	S	0.999		930			
194	M	1.000		931			
195	H	1.000		932			
196	D	0.916		933			
197	L	0.997		934			
198	V	1.000		935			
199	G	0.991		936			
200	G	0.947		937			
201	L	1.000	1	938			
202	L	1.000		939			
203	Q	0.907		940			
204	F	1.000	1	941			
205	C	1.000		942			
206	F	1.000		943			
207	Y	0.988		944			
208	T	1.000	1	945			
209	F	1.000		946			
210	V	0.914		947			
211	Q	0.807		948			
212	S	1.000		949			
213	Q	0.717		950	K	0.28	skateMR, skateGR
214	A	0.958		951			
215	L	1.000		952			
216	S	0.955		953			
217	V	0.998	1	954			
218	E	1.000		955			
219	F	1.000	1	956			
220	P	1.000		957			
221	E	0.997		958			
222	M	1.000		959			
223	L	0.989		960			
224	V	0.697		961	A	0.29	lampreyCR
225	E	1.000		962			
226	I	1.000		963			
227	I	1.000		964			
228	S	0.996		965			
229	D	0.703		966	N	0.25	skateGR
230	Q	1.000		967			
231	L	1.000		968			
232	P	1.000		969			
233	K	0.997		970			
234	V	0.906		971			
235	M	0.362		972	T	0.23	skateMR
236	A	0.838		973			
237	G	1.000		974			
238	M	0.925		975			

239	A	0.911	976
240	K	1.000	977
241	P	0.991	978
242	L	1.000	979
243	L	0.988	980
244	F	1.000	981
245	H	1.000	982
246	K	0.913	983
247	K	1.000	984

mean		0.938	
------	--	-------	--

Table S3. Amino acid sequence identity of AncCR to extant receptors in the ligand-binding domain (LBD, which includes the carboxy-terminal extension) and in the residues predicted to form the hormone-contacting residues of the ligand-binding pocket (LBP) based on crystallography of the human MR (8). Aldosterone-sensitive receptors in bold. Ranked by similarity in the LBP.

	LBP	LBD
SkateMR	0.95	0.80
AstatotilapiaMR	0.95	0.78
SkateGR	0.95	0.76
HumanMR	0.95	0.75
HagfishCR	0.86	0.63
AstatotilapiaGR1	0.82	0.70
LampreyCR	0.77	0.66
HumanGR	0.77	0.66

Table S4. Effects of GR-diagnostic residues on ligand activation of AncSR4-LBD. Sites in the protein sequence that change on the branch leading to the GRs of bony vertebrates, with one conserved state in all aldosterone-activated corticosteroid receptors and another state in all aldosterone-insensitive receptors, were introduced singly and in combination into the AncSR4 background. These were then assayed in a luciferase reporter gene assay. The double mutant S106P/L111Q (bold) produced a GR-like phenotype, with a radical reduction in sensitivity to aldosterone, while moderate cortisol activation was retained. Some others showed large reductions in aldosterone responsiveness, but cortisol activation was also knocked out.

Receptor LBD	Aldo EC50	Cortisol EC50
RatGR	>1000	64
AncSR4	0.23	5.7
AncSR4 S106P/L111Q	148	72
AncSR4 L29M	2.1	72
AncSR4 F98I	71	>1000
AncSR4 S106P	70	>1000
AncSR4 L111Q	1.7	9.2
AncSR4 L29M / F98I	>1000	>1000
AncSR4 L29M / S106P	355	>1000
AncSR4 L29M / L111Q	12.5	62
AncSR4 F98I / S106P	>1000	>1000
AncSR4 F98I / L111Q	96	513

REFERENCES FOR SUPPLEMENTAL INFORMATION

1. J. W. Thornton, *Proc Natl Acad Sci U S A* **98**, 5671 (2001).
2. S. Green, P. Chambon, *Nature* **325**, 75 (1987).
3. H. Takahashi *et al.*, *Int J Pept Prot Res* **46**, 197 (1995).
4. J. D. Thompson, D. G. Higgins, T. J. Gibson, *Nucleic Acids Res* **22**, 4673 (1994).
5. F. Ronquist, J. P. Huelsenbeck, *Bioinformatics* **19**, 1572 (2003).
6. Z. Yang, S. Kumar, M. Nei, *Genetics* **141**, 1641 (1995).
7. J. A. Ugalde, B. S. Chang, M. V. Matz, *Science* **305**, 1433 (2004).
8. J. Fagart *et al.*, *Nat Struct Mol Biol* **12**, 554 (2005).